Chapter 2
Background

2.1 Topical Drug Delivery

2.1.1 Structure of the Skin

The principal role of skin is to act as a barrier against evaporative water loss and against the entry of harmful foreign agents. The protective role of the skin is accomplished by its layered structure. The basic layers of human skin (outlined in Fig. 2.1a) consist of the hypodermis, epidermis and dermis. The hypodermis (up to several millimetres thick across the body) is made up of a network of fat cells and plays an important role in energy storage and metabolism [1]. It also provides protection against injury. The dermis, with thickness in the range of 0.3–3 mm, lies above the hypodermis and forms the bulk of the skin [2]. It is primarily composed of collagenous fibres and elastic connective tissue. This layer determines the elasticity of the skin and provides the physical support needed for networks of nerves and blood vessels [1, 3].

The epidermis (60–800 μm thick) contains distinct layers which are commonly categorised into the stratum corneum (SC), the uppermost layer, the stratum granulosum, the stratum spinosum and the stratum basale, the latter of which forms the lowest layer [3]. The viable epidermis, comprising of all layers apart from the SC, is primarily responsible for the formation of the SC and also contains melanocytes, which produce melanin for ultraviolet (UV) absorption, and Langerhans cells, which are responsible for the immune response of the skin [4]. After cell division in the stratum basale, cells migrate upwards towards the skin's surface. During this migration, the cells undergo differentiation, flattening and losing their nucleus. The SC is composed of approximately 10–15 layers of differentiated cells and this thin layer, up to approximately 30 μm thick, provides the majority of the skin's barrier function.

H. Garvie-Cook, *Novel (Trans)dermal Drug Delivery Strategies*,
Springer Theses, DOI 10.1007/978-3-319-28901-4_2

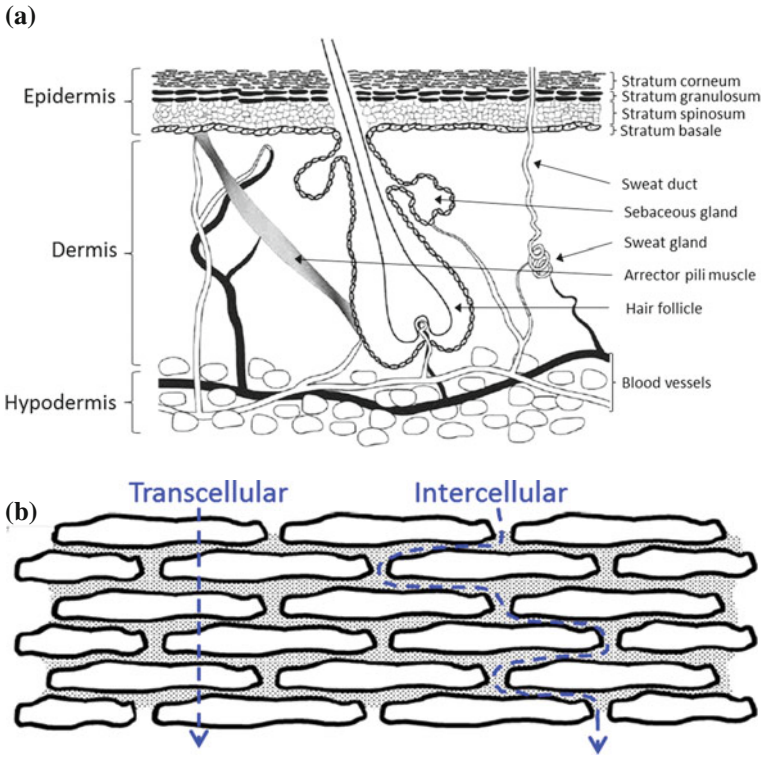

Fig. 2.1 **a** The structure of human skin. Image adapted from [3]. **b** The structure of the SC can be described using a "bricks and mortar" analogy. The corneocytes (in *white*) and the intercellular lipids (continuous domain in *dots*) represent the bricks and mortar, respectively. Two routes contributing to the percutaneous absorption of topically applied compounds, the transcellular and intercellular routes, are shown

2.1.1.1 Stratum Corneum

The SC has a "bricks and mortar" structure (Fig. 2.1b) of dead, anucleate cells, termed corneocytes, surrounded by a lipid matrix [5]. The SC comprises approximately 96 % proteins and water and 4 % lipids [6]. Corneocytes are primarily composed of bundled keratin surrounded by an envelope of cross-linked proteins and lipids. These flat, polygonal cells are typically 0.2–1.5 μm thick and have diameters of approximately 30–50 μm [3]. The composition of the intercellular lipids varies according to the individual and the anatomical site, but it mostly constitutes ceramides, fatty acids and cholesterol [7]. Corneodesmosomes are proteinaceous structures which connect corneocytes and contribute to the cohesion of the SC [1]. The hydration of the SC is maintained by the so-called natural moisturizing factor, a highly water soluble mixture of amino acids, derivatives thereof, urea and specific salts [8].

The barrier provided by the SC is influenced by physiological factors and skin disease. Age-related changes to the structure of the SC include the maturation of the underdeveloped premature neonatal skin [9] and an increase in corneocyte area and a decrease in SC thickness with increasing age [1]. Skin diseases, such as psoriasis and dermatitis, can affect both the protein and lipid composition of the SC, influencing and disrupting its barrier function [10]. UV exposure, hydration and chemical assault, amongst others, also affect the SC's barrier [3].

2.1.2 Topical Medication

Topical delivery refers to the application of formulations to the surface of the skin for the delivery of therapeutic agents (also known as drug substances) to pathological sites within the skin (dermal delivery) or through the skin into the blood stream and systemic circulation (transdermal delivery). Examples of dermatological conditions which are treated using dermal delivery are psoriasis and eczema [3], while the treatment of severe pain with fentanyl is an example of transdermal delivery [11]. In conventional topical therapy for dermatological disease, the drug is incorporated into a vehicle, such as a cream, which facilitates the application of the formulation and the delivery of the drug to the required site. The non-drug components of the formulation are termed excipients. The efficacy of topical delivery depends on the formulation and the diffusion of the therapeutic agent through the skin.

Transdermal and dermal routes of administration are advantageous in several aspects when compared, for example, to oral and intravenous delivery. For the oral treatment of skin disease, the systemic concentration of the drug must be high enough to achieve therapeutic benefit at the diseased site. In contrast, a lower dose is needed for a formulation that is applied directly to the affected site of the skin, decreasing or eliminating any adverse effects of the drug [12]. Transdermal delivery also avoids first pass metabolism of the drug, which decreases its concentration [13], allowing for a lower daily dose. Oral delivery involves a peak of drug concentration in blood and tissue, followed by a decline. (Trans)dermal delivery, however, can maintain drug level within the therapeutic window for a prolonged period of time, extending the duration of the action of the drug and reducing the frequency of dosing required. In the case of patches, the drug input can be terminated simply by removal of the patch.

2.1.2.1 Permeation Pathways

There are three main pathways by which drugs can permeate the SC: via the appendages (appendageal), through intercellular domains (intracellular) and through the cells themselves (transcellular) (Fig. 2.1b). The contributions of these three routes to the percutaneous absorption of a topically applied compound, from the surface of the skin either into the skin or into systemic circulation, depend on the nature of

the permeating molecules and the density of appendages, such as hair follicles and sweat ducts, at the site of application [1].

Appendages penetrate the SC and the epidermis, providing a route for permeation which "bypasses" the barrier. The density of appendages varies, depending on the anatomical site, but is consistently low. This relatively low resistance route of transport plays a large role in iontophoris and is thought to be quite important for compounds of low SC diffusivity, such as hydrophilic and large molecular weight compounds [3].

The transcellular route requires the repeated penetration of the permeating compound into and out of the corneocytes and the intercellular lipids. In this route of permeation, the compound must therefore diffuse through both lipophilic regions (lipids) and hydrophilic regions (hydrated keratin within corneocytes) of the SC.

The major pathway for the permeation of small ($<500\,\mathrm{g\,mol^{-1}}$ [14]), uncharged molecules is believed to be intercellular [3]. Intercellular lipids, providing the only continuous phase within the SC, form lamellar structures between corneocytes. The permeation of compounds via this route is thought to occur by diffusion along and/or across lipid lamellae [1] which provide the rate limiting step [15].

2.1.2.2 Diffusion

Drug transport across the SC occurs by passive diffusion and can be described by Fick's first law [3],

$$J_{max} = \frac{D K_{SC/V} {C_V}^{sat}}{h} \tag{2.1}$$

where J_{max} is the maximum flux of the permeant, D is its diffusion coefficient in the barrier (typically the SC), $K_{SC/V}$ is the partition coefficient of the permeant between the SC and the vehicle, ${C_V}^{sat}$ is the saturation concentration of the permeant in the vehicle, and h is the diffusion pathlength. The diffusion coefficient measures how easily the permeant traverses the SC, while $K_{SC/V}$ describes the distribution of the permeant between the SC and the vehicle, and reflects the ratio of the compound's solubilities in these two phases,

$$K_{SC/V} = \frac{{C_{SC}}^{sat}}{{C_V}^{sat}} \tag{2.2}$$

where ${C_{SC}}^{sat}$ is the saturation concentration of the permeant in the SC. Under ideal circumstances, therefore, J_{max} is independent of the vehicle at its saturation concentration, assuming that the vehicle does not alter the properties of the SC or the permeant solubility in the SC. The diffusivity D of the drug through the SC can be altered by the diffusion of the vehicle's components into the SC, and the effect of this on the drug's solubility, and can be increased by incorporating an enhancer into formulations. The use of enhancers, however, may produce skin irritation. Drug flux

can be maximised via the SC-vehicle partition coefficient and the concentration of the drug in the vehicle.

2.1.2.3 Formulation Considerations

The design and constituents of the formulation influence the onset, extent and duration of therapy. Topically applied formulations must both be cosmetically acceptable, to ensure patient compliance, and must also maximize the bioavailability of the drug in the formulation; that is, the fraction of the administered dose which reaches the target tissue and the rate at which it gets there. Topically applied formulations include creams, ointments, gels and lotions (all semi-solid), as well as transdermal patches (solid state). In the design of an effective formulation, the following must be taken into account: the physico-chemical properties of the incorporated drug, the stability of the excipients and the drug substance, and the cosmetic acceptability of the formulation (good feel on the skin, appropriate texture and fragrance) [3].

Examples of materials which are commonly used as dispersive media in the preparation of semi-solid formulations are oils and fats (e.g. petrolatum and triglycerides) and hydrogels (usually water and/or alcohol based). These ingredients are often included to stabilise, adhere, dilute or thicken the formulation [1]. Solvents form the basis of the formulation and a commonly used example is water, which is non-irritating and solubilises a wide range of compounds. Transdermal patches contain the drug within an adhesive layer or a (typically polymeric) matrix. The rate of delivery can be modified by varying the composition and structure of the patches.

Increasing the concentration of a compound within a vehicle increases the rate of its release (Eq. 2.1). The selection of a vehicle, however, is a compromise between the solubility of the compound and the SC-vehicle partition coefficient. If a vehicle is altered to make a compound more soluble, the SC-vehicle partition coeffiecient decreases (Eq. 2.2) and the "leaving tendency" of the drug from the vehicle is low. At saturation, the release of the compound from the formulation is generally maximum [1]. Below saturation, the rate of release of the compound is greatest for the vehicle in which it is least soluble (having the highest "leaving tendency"). Increasing the concentration of the drug above its saturation results in the formation of a suspension of the drug and smaller fractions of the compound are in solution. The period over which delivery at the maximum flux (provided by the solubilised drug within the oversaturated vehicle) is maintained becomes shorter, as the dissolution of crystalline material in the vehicle limits this process.

The stability of the drug within the formulation (the ability of the drug to maintain therapeutic properties during storage and use) is related to its solubility in the vehicle. Consideration of the metamorphosis of formulations post-application is vital: solvent loss through evaporation and/or uptake into the SC results in an increase of the concentration of the compound in the remaining formulation. This potentially leads to the formation of solid drug particles or crystals which are unlikely to be absorbed to the target site in the skin [16].

2.1.3 Polymeric Film-Forming Systems

Polymeric film-forming systems (FFS) are a potentially advantageous approach to topical delivery. Thin and nearly-invisible films are formed in situ on the skin upon application of the FFS and subsequent solvent evaporation. FFS comprise primarily a polymer, a drug substance and a volatile solvent, but may also include other excipients such as plasticizers and/or lipids [17, 18].

Polymeric FFS have previously been used, for example, as tissue glue for thread-free closing of incisions [19], as a preoperative skin preparation [20], and in ostomy care [21]. FFS for transdermal drug delivery of steroidal hormones [22, 23] and analgesics [24, 25] have been reported but there is limited literature describing their use in dermal delivery. Frederiksen et al. assessed the in vitro release of betamethasone-17-valerate (BMV), used in the treatment of inflammatory skin conditions, from polymeric films of varying compositions [18]. Release from the films was found to depend on the nature of the polymer and the incorporated plasticizer.

FFS present potential advantages over conventional dosage forms, such as higher dosing flexibility and better patient compliance [26]. While the area of a patch is fixed, that of a film can be determined by the patient, allowing flexible and complete coverage of the affected/target site. The nearly invisible appearance of the films renders them less noticeable and their rub off resistance and fast drying times are more acceptable than those of semi-solid preparations, such as creams [27].

2.1.3.1 Film Composition

Suitable polymers for the fabrication of film-forming systems must form clear, flexible films at temperatures close to that of the surface of the skin (approximately 28–32 °C). These film-forming polymers must also be soluble in a skin-tolerant, volatile solvent.

Increasing the polymer content of a film typically means that more drug can be incorporated. However, this means that the film becomes more viscous. While this is manageable up to a point, the viscosity must not be so high that the film's application from a spray is prevented [26].

Addition of plasticizer to the films increases their flexibility and their ability to "move" with the skin [26, 28]. More flexible films are less likely to crack, meaning that a constant area for drug transport is maintained over a prolonged period of time. Increasing plasticizer content also increases the adhesion of polymeric films [26], but can make them sticky on their outer surface. The type of plasticizer incorporated influences drug release from polymeric films [18, 29], as do other additives, such as lipids [17, 30] or penetration enhancers [26].

2.2 Atomic Force Microscopy

Atomic force microscopy (AFM) provides a 3D profile of the surface of a sample using forces between the sharp tip of an AFM and the sample surface. The probe tip is attached to the end of a sensitive cantilever. As the tip is scanned over the sample, the cantilever deflects according to the topography of the surface. A diagram of a basic AFM is shown in Fig. 2.2.

The main components of an AFM are a microscope stage (including the scanner, sample holder and a force sensor), control electronics and a computer. Typically, the cantilever deflection is measured using the reflected signal of a laser beam from the back of the cantilever. The laser is reflected to a four quadrant photodiode, which monitors the position of the beam by changes in its output voltage. Cantilevers are microfabricated from silicon or silicon nitride using photolithography techniques; probe tips typically have radii of curvature on the order of nanometers.

A piezoelectric device is used to adjust the vertical z position of the sample according to the feedback system being used. The sample is moved in the x, y plane using other piezoelectric devices. It is the z position of the sample, as a function of its x, y position, which forms the topographical AFM image.

There are several advantages of using the AFM over more conventional imaging approaches, such as light microscopy and scanning electron microscopy, especially for biological samples. Minimal treatment is required prior to imaging using the AFM, meaning that staining, labelling and coating of samples is avoided, minimizing damage to and alteration of the sample. Damage is also minimised in tapping

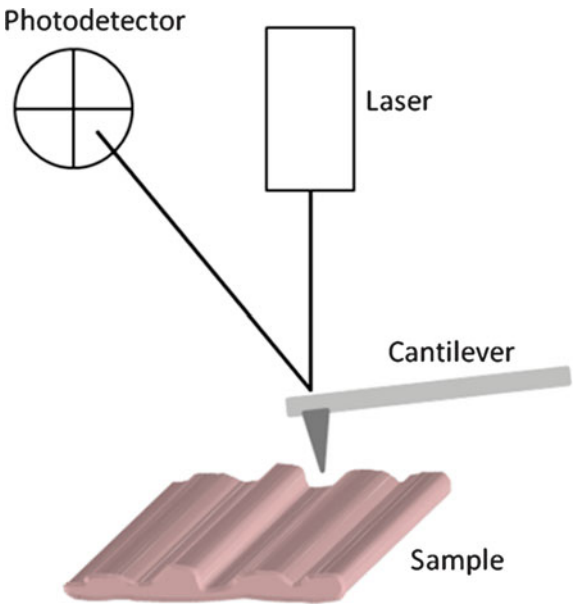

Fig. 2.2 Basic set-up of an AFM. The cantilever deflects according to interactions between the probe tip and the sample. This deflection is measured using the reflection of a laser beam from the back of the cantilever to a four quadrant photodiode

mode AFM imaging, further discussed in Sect. 2.2.1. The AFM produces 3D images, allowing for the entire surface structure of the sample to be better characterised. In addition, AFM can be used in physiologically relevant environments, facilitating live cell imaging and investigation of real time biological events at the nanoscale.

The major limitation of the AFM is its scan range, which is no more than approximately $100 \times 100\ \mu m^2$ in the x and y directions, and about $10\ \mu m$ in the z direction. The analysis of samples with roughness on or larger than this scale, such as skin, is therefore limited to rather small areas.

2.2.1 Operating Modes for Imaging

In contact mode AFM, the probe tip is always in contact with the sample. The cantilever is directly deflected by the surface of the sample and low stiffness cantilevers are used to maximise the deflection signal. A feedback system within the AFM corrects the height of the probe tip above the sample such that the cantilever deflection is maintained at a predetermined value, the set-point. The image of sample height is created from this change in cantilever height. Contact mode is most successful on stiff samples which do not deform under the load applied by the probe tip. However, the normal load from the tip and also the lateral force can distort and damage softer samples. Contact mode is also the most easily applied topographical mode when imaging samples in liquid [31].

There are several dynamic modes of operation where the cantilever is driven to oscillate, typically at its resonance frequency. As the oscillating probe approaches the sample, the interaction between the probe tip and the sample surface changes the frequency and amplitude of the oscillation. A feedback loop changes the height of the sample to maintain the amplitude or frequency of oscillation. It is from this change in height that a topographical image is acquired.

Intermittent-contact mode AFM is commonly used in ambient conditions. In this topographical mode, the cantilever is oscillated with a relatively large amplitude (1–100 nm), such that the tip and sample touch each other during each oscillation. The feedback system usually maintains the amplitude of the oscillation. As the cantilever is oscillated perpendicular to the surface of the sample, and the majority of the oscillation is out of contact with the sample, lateral forces are almost eliminated, making this an ideal topographical mode for imaging soft samples.

2.2.2 Nanoindentation

The AFM was designed initially as an imaging system, but the usefulness of the force sensitivity of the AFM cantilever has since been utilized in nanoindentation. In this technique, the response of the probe tip is recorded as it indents the sample. Material properties such as elastic modulus and hardness can be calculated at a spatial

resolution limited by the size of the probe. Nanoindentation can also be carried out using dedicated apparatus but these measurements are usually on a larger scale with lower force sensitivity. AFM nanoindentation can be used to measure properties in thin and heterogeneous samples at the nanoscale. The interpretation of AFM nanoindentation data is further discussed in Sect. 3.1.3.

2.2.3 AFM Imaging and Nanoindentation in Pharmaceutics

The versatility of the AFM has facilitated the investigation of a large range of samples, such as metals, polymers, glasses and biological materials [31]. Little sample modification is required for AFM analysis and samples can be contained within physiologically relevant environments, meaning that this technique has proved extremely useful in the analysis of materials relevant to the pharmaceutical industry, including devices and drug particles.

Examples of the use of AFM for the analysis of pharmaceutical samples include investigation of the effects of humidity on spray-dried lactose that elucidated the process of crystallization [32]. The adhesion between lactose spheres and between compressed powder discs of lactose has also been used to predict the dispersion of these particles when delivered using dry powder inhalers [33]. Strong forces between particles have been shown to decrease the efficiency of these devices. The AFM has also been used to determine the size distribution of crystalline drug nanoparticles [34]. The resolution of the AFM permitted the detection of nanoparticles smaller than 40 nm in diameter (which are not detectable with the light scattering techniques commonly used). In these experiments, the AFM also provided information on the shape and structure of the nanoparticles that influence dosage performance. AFM imaging and nanoindentation have been used complementarily to distinguish nanoscale amorphous and crystalline domains on the surface of discs of crystalline sorbital (a commonly used excipient) [35]. The mechanism of drug release from solid lipid nanoparticles (SLN), during in vitro dissolution tests, was investigated using AFM imaging and nanoindentation [36]. Identification of soft, non-crystalline layers, surrounding the solid lipid core, was achieved by repeatedly imaging the particles. The particles appeared to spread out in this process, a phenomenum that was attributed to the deformation of the softer, outer layers by the AFM probe tip. Nanoindentation revealed the thickness of these outer layers and the initial, fast release of drug was explained by this softer, hydrophilic, non-crystalline outer layer.

Understanding the mechanics of the skin is useful for fully optimising topically applied drug delivery systems or devices for porating the skin. Solid-state dosage forms, such as the polymer films investigated in this work, ideally behave similarly to the skin when formed in situ on its surface. In this way, the two will flex together and remain in intimate contact for a prolonged period of time. The mechanical properties of the skin have previously been studied using cylindrical flat punches with radii ranging from 0.5–20 μm [37]. Elastic moduli extracted from these measurements decreased with increasing radius of the indenter. This was thought to be due to

the softer, lower layers of skin bearing the load on the stiffer, uppermost layers. The elastic modulus extracted for the smallest radius probe (closest to the indenter geometry used in this work) was 0.03 (±0.02) GPa. The mechanical properties of corneocytes as a function of the depth from the SC surface were determined using nanoneedle AFM probes, with diameters between 30 and 80 nm [37]. This high resolution study of the mechanical structure of corneocytes revealed stiffer structures from within the cells and was predicted to be of value in the detection of disease-related changes in cells and the effects of, for example, UV exposure. The elastic modulus at indentations below 100 nm (surface elastic modulus) was approximately 0.3 GPa.

The effect of applying a commercially available moisturiser on the nanomechanics of skin has been determined [38]. The resistance of the skin to a scratch from an AFM probe tip was investigated and elastic moduli before and after the application of this skin cream were 0.09 (±0.03) and 0.05 (±0.02) GPa, respectively. The effect of moisturizer on individual corneocytes, isolated using tape stripping, has also been investigated and the surface roughness and elastic modulus of the cells shown to decrease [39].

2.3 Raman Spectroscopy

Raman spectroscopy yields information on molecular vibrations. These vibrations are sensitive to the strength and types of chemical bonds in the sample. Raman spectra can therefore be used to identify substances and help to elucidate their structures.

Raman spectroscopy is based on the scattering of incident light by molecules within a sample [40] (Fig. 2.3). Photons from the excitation light collide with molecules within the sample either elastically, without changing their energy (Rayleigh scattering), or inelastically, exchanging energy in the process (Raman scattering). When energy is exchanged, in Raman scattering, the molecule is excited to a virtual energy state. The molecule undergoes a transition from this virtual state to a lower energy state, which differs from its original state, and emits a photon.

If the frequency of the scattered photon is lower than that of the incident photon, the interaction is termed Stokes Raman scattering. Anti-Stokes scattering occurs

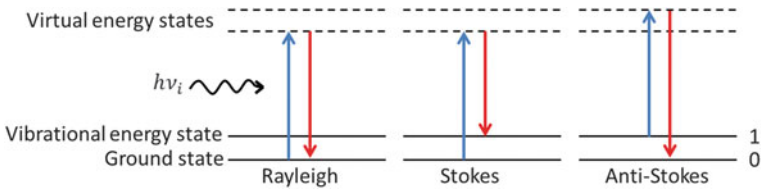

Fig. 2.3 Energy level diagrams showing Rayleigh and Raman (Stokes and anti-Stokes) scattering on excitation by a photon with energy $h\nu_i$

when the emitted photon has a higher frequency than the incident one. A molecule must be initially in an excited state for anti-Stokes Raman scattering to occur. Stokes Raman scattering arises from the interaction between a photon and a molecule in its ground state. Molecules are usually in their ground state at room temperature, so Stokes occurs more frequently than anti-Stokes scattering and is therefore more frequently used for spectroscopy.

The frequency shift of photons associated with their inelastic collisions is called spectral shift. A Raman spectrum shows the intensity of scattered radiation as a function of spectral shift and the intensity is directly proportional to the concentration of the scattering species [41].

Major components of a Raman spectrometer are the excitation source (a laser), the spectrometer, the detector and the optical set up [40]. The choice of laser depends on the sample being analysed. The use of particular wavelengths may excite strong, broad fluorescence in the samples, which can overwhelm the Raman signal. At higher excitation wavelengths, fewer fluorescent sources are excited but the intensity of Raman scattering is lower [42]. If samples are unlikely to fluoresce, shorter wavelengths in the visible range are usually employed, requiring a lower laser power and therefore reducing the likelihood of sample damage.

Raman spectroscopy is commonly compared to IR spectroscopy, which is based on the absorption, reflection and emission of light, as opposed to scattering. The two techniques can be used to provide complementary spectral information. In other instances, one technique may be preferred. For example, water has a weak Raman signal and does not interfere with the measurement of spectra from aqueous solutions [41]. The strong IR spectrum of water, however, may overwhelm the spectral information of the other components of an aqueous solution. The lateral spatial resolution of Raman spectroscopy is about 10-fold better than that of IR, (1 μm vs. 10 μm), facilitating the analysis of finer structure [43].

2.3.1 Raman Chemical Mapping

Chemical imaging combines spectroscopic techniques with optical microscopy. Spectra are acquired across the sample at predefined points. The total number of spectra in the map (corresponding to the total number of pixels) depends on the area of the map and the area over which individual spectra are acquired. High quality chemical maps are achieved using long exposure times and the acquisition of a large number of spectra. The collected spectra form a chemical image in which, for example, the concentration and the form of the constituents of the sample can be mapped. When analysing the data and forming a map, there is ideally at least one distinct peak for each of the constituents being mapped.

2.3.2 Raman Spectroscopy in Pharmaceutics

Since the development of instrumentation for Raman micro-spectroscopy, the method has been used, for example, to provide information on the homogeneity of the distribution of drug and excipients within a sample. This was demonstrated by mapping the distribution of estradiol within transdermal patches [44]. An inclusion of crystalline estradiol was observed ($\sim$250 μm in size), which was expected to negatively influence delivery and therefore compromise the efficacy of the patch. The distribution of drug and excipient within pharmaceutical tablets has also been shown [45], and related to the release rate. Raman spectroscopy has also been used to determine the physical state of a drug within its vehicle using the position, intensity and shape of characteristic spectral bands [46].

2.4 Laser Poration

The careful design of topically applied formulations can ensure the adequate delivery and therapeutic benefit of low molecular weight compounds. However, the penetration of compounds with molecular weights above 500 g mol^{-1}, for example vaccines and peptides, is severely limited by the SC barrier, regardless of formulation optimisation [14]. This is unfortunate in the case of vaccines because their delivery into viable skin is expected to elicit a more efficient immune response than that seen when they are injected subcutaneously or intramuscularly [47, 48]. It has therefore been argued that this deficiency, as well as mitigating the risks associated with injections, such as needle re-use and pain, might be avoided by delivery through porated skin, the SC of which has been superficially ablated with a laser, for example. Such an approach would also enhance the delivery of small molecular weight compounds [49].

2.4.1 SC Penetration Enhancement Methods

The SC barrier may be circumvented, at least partially, by formulation optimisation, energy driven approaches, minimally invasive technology and SC removal [50]. The latter can be achieved using radio-frequency ablation, laser microporation and thermal ablation, for instance [51].

Microporation using laser irradiance to ablate the SC provides several potential advantages. It is a needle-free technique, which does not produce bio-hazardous waste, and has been reported to be relatively painless [52]. The same device for poration can be used repeatedly, in contrast to the use of microneedle patches, for example. The area and depth of ablated pores depend on laser power and its delivery to the skin, ensuring that the approach is controllable and predictable [47, 53].

Furthermore, by limiting thermal damage to a small area, the pores produced heal quickly [47]. Devices are currently available to produce micropores in the skin and enhance the delivery of topically applied drugs [54, 55].

2.4.2 Laser Ablation

Tissue ablation is any process of tissue incision or removal. Laser ablation of skin is the removal of tissue by laser irradiance. The mechanism by which the tissue is removed depends on the wavelength and pulse duration of the laser used and on tissue characteristics [56]. There are three major models of tissue ablation by short laser pulses: selective photothermolysis and its variations (photothermal and photomechanical); photochemical; and plasma-mediated [57]. Earlier investigations of tissue ablation used lasers with nanosecond or greater pulse lengths, for which photothermal and photomechanical mechanisms (when visible or infrared wavelengths were used [58, 59]) or a photochemical mechanism (in the case of UV ablation [60]) were believed to occur.

Photothermal ablation is achieved by rapid heating of a target chromophore within the tissue [61]. Chromophores are components of tissue which absorb a specific wavelength of light and examples include collagen, melanin and water [56]. The target chromophore absorbs laser radiation and heats the water in the surrounding tissue. The subsequent vaporization of the water leads to a build-up of pressure within the tissue and a micro-explosion occurs, which ablates material from the surroundings [48]. In the case of short laser pulses, their duration can be less than the thermal relaxation time of the targeted tissue component, resulting in little heat transfer, and therefore less damage, to the surrounding tissue [62]. Tissue can also be ablated photomechanically, when the stress induced by laser heating exceeds the strength of the material. This leads to ejection of tissue fragments [63].

In photochemical ablation, the removal of tissue also results from explosions caused by the build-up of pressure. The pressure in this case derives from the photochemical dissociation of macromolecular bonds [60]. For far-UV (<200 nm) laser irradiation, the photon energy is larger than that of the chemical bonds in the molecule [64] and absorption of photons provokes electronic excitation and subsequent decomposition of the tissue into smaller, volatile fragments.

For pulse lengths in the range of picoseconds to femtoseconds, plasma-mediated ablation has been proposed [56, 65, 66]. Laser induced breakdown is one mechanism for creating plasmas. In this process, the tissue under irradiance is partially or completely ionized through absorption of laser energy and this results in a “gas” of charged particles, a plasma [67]. Plasmas absorb optical radiation much more strongly than ordinary matter and therefore limit the penetration of the incident light [68]. Once the pulse has terminated, free electrons recombine with the positively ionized molecules within the plasma and energy is transferred to surrounding material which is ablated. The energy from this recombination can also be converted to

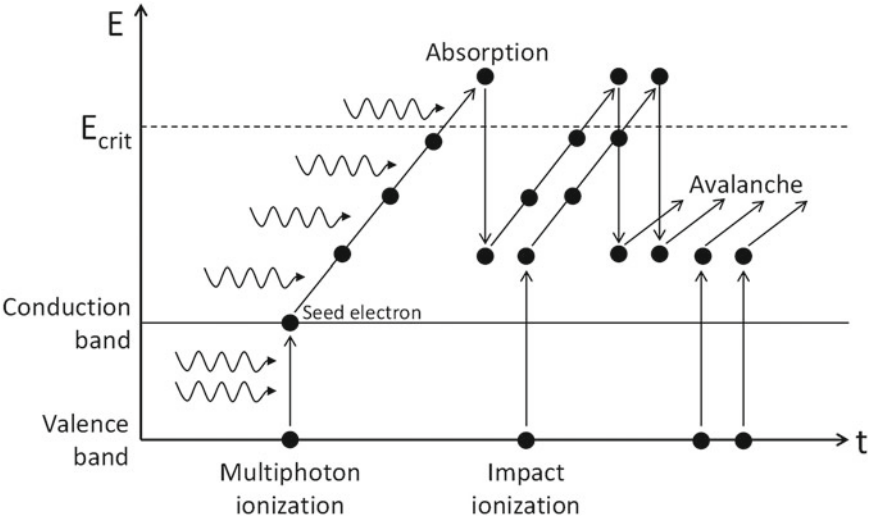

Fig. 2.4 Multiphoton ionization, absorption and impact ionization leading to an avalanche growth in the number of free electrons and the formation of plasma. E_{crit} is the critical electron energy for impact ionization to occur. Adapted from [66]

mechanical energy, resulting in the propagation of a shock wave and the formation of a cavitation bubble [69].

An initial threshold electron density must be reached for the formation of the plasma, and the threshold for laser induced breakdown is an electron density of 10^{18}–10^{20} cm^{-3} in the focal volume [65]. Two mechanisms can produce electron densities in this range (Fig. 2.4): (i) avalanche (or cascade) ionization, initiated either by seed electrons from impurities or by multiphoton absorption, and (ii) pure multiphoton ionization.

Free electrons are required in the focal volume for avalanche ionization to occur [65]. These "seed" electron(s) absorb photons, accelerate and then release bound electrons by collisional ionization. The freed electrons are then accelerated, freeing more electrons and the avalanche process continues, resulting in the formation of plasma. The "seed" electrons required for this process may come from easily ionized impurities or from multiphoton ionization.

Multiphoton ionization occurs when electrons are freed by absorption of multiple photons. High electron densities are produced by pure multiphoton ionization when pulse lengths are in the low femtosecond range [65] so only instantaneous ionization can occur in the duration of the time that the pulse is present in the focal volume. Each atom is independently ionized so no seed electrons, collisions or particle-particle interactions are required.

2.4.3 Laser Poration of Skin

The potential of lasers in biomedical applications was realised soon after the invention of the pulsed ruby laser in 1960 [70]. It was predicted that lasers could provide previously unachievable precision and selectivity in the manipulation of tissues [71]. Within a couple of years, the effect of exposure of skin to a pulsed ruby laser beam had been investigated. Goldman et al. [72] exposed non-pigmented and pigmented rabbit and human skin to a pulsed ruby laser beam (λ = 694.3 nm) with a pulse length of 200 μs and observed an enhanced interaction between the laser and the pigmented skin. Subsequent experiments showed that tissue changes were related to the skin pigmentation, the type of laser used, the fluence (the energy per unit area per exposure) and the duration of the exposure to the laser beam [73, 74]. The possible treatment of birthmarks (nevi), melanomas and tattoos, based on these findings, was proposed [75].

The first demonstration of controlled removal of the SC to enhance percutaneous transport was in 1987 [76]. In this study, an excimer laser was used (λ = 193 nm) with a pulse length of 14 ns. An unexpected decrease in permeation when using a higher laser fluence to remove the SC was observed, however, even though similar amounts of material were removed. It was concluded that tissue damage and cauterization occurred when a higher fluence was used, due to the build-up of heat. Ideally, for drug delivery applications, the pore created would not be surrounded by coagulated tissue, as this effectively blocks subsequent permeation through the pores [54].

Shortly thereafter, it was demonstrated that nanosecond pulsed lasers, with wavelengths strongly absorbed by the water in the skin, caused much less thermal damage of the surrounding tissue [77, 78]. Since then, a range of laser systems have been used for SC removal, as illustrated in Table 2.1.

Over the last 25 years, laser ablation of skin has focussed on the wavelengths of 10,600 and 2940 nm, produced using CO_2 and Er:YAG lasers, respectively. This causes ablation of the skin photothermally using the pulse durations reported in Table 2.1. Here, conventional ablation refers to the use of just one, large (mm in size) pore for drug permeation enhancement or cosmetic benefit (such as skin resurfacing or wrinkle treatment [93]). The use of these lasers, however, was associated with delayed re-epithelialisation and erythema (skin redness), with long recovery times of the large wounds produced [94].

Fractional photothermolysis, first described in 2004 [95], involves the use of a split laser beam to create an array of micropores in the skin. Fractional lasers are advantageous in that they create smaller zones of damage, within the surrounding, healthy skin, that are quicker to heal [82, 87].

The hand-held P.L.E.A.S.E.® device (Precise Laser Epidermal System), developed by Pantec Biolsolutions AG (Ruggell, Liechtenstein), uses a fractional Er:YAG laser to create micropores in the skin for both drug delivery enhancement [47, 53, 83–86] and cosmetic procedures [96]. The number of pores and the fluence used to create the pores are specified prior to the use of the device, enabling the distribution

Table 2.1 Illustrative articles reporting laser ablation of skin to enhance the permeation of topically applied substances

Year	Laser (wavelength, pulse duration)	in vitro/in vivo	Drug/permeant
1987	Conventional excimer (193 nm, 14 ns)	in vitro, human	Tritiated water [76]
1991	Conventional Er:YAG (2970 nm, 250 μs)	in vitro, porcine	Hydrocortisone[a], interferon[b] [58]
2002	Conventional ruby (694 nm, 40 ns), Er:YAG (2940 nm, 250 μs), CO_2 (10,600 nm, 50 ms)	in vivo, murine	5-Fluorouracil[c] [79]
2006	Conventional Er:YAG (2940 nm, 600 μs)	in vivo, human	Lidocaine[d] [80]
2008	Conventional Nd:YAG (1064, 532 and 355 nm, pulse durations of 11, 11 and 18 ns, respectively)	in vitro, rabbit	5-Fluorouracil[c] [81]
2010	Fractional and conventional Er:YAG (2940 nm, 350 μs)	in vitro, porcine	ALA[e] [82]
2010–2013	Fractional Er:YAG (P.L.E.A.S.E.®, 2940 nm, pulse duration unknown but photothermal ablation reported)	in vitro/in vivo, porcine, murine and human	Lidocaine[d] [83], prednisone[f] [53], ovalbumin[g] [47], diclofenac[h] [84], antibodies (ATG and basiliximab)[i] [85], Proteins (12.4–70 kDa) [86]
2010	Fractional Er:YAG (2940 nm, 400 μs)	in vitro/in vivo, murine/porcine	ALA[e] [87]
2010	Fractional CO_2 (10,600 nm, 3 ms)	in vitro/in vivo, porcine	Methyl ALA[e] [55]

(continued)

Table 2.1 (continued)

Year	Laser (wavelength, pulse duration)	in vitro/in vivo	Drug/permeant
2011	Conventional frequency doubled Nd:YAG (532 nm, 11 ns)	in vitro, rabbit	ALA[e] [59]
2012	Fractional CO_2 (10,600 nm, 6 ms)	in vitro, human	Polyethylene glycols (240–4300 Da)[j] [88]
2012	Fractional CO_2 (Ultrapulse, 10,600 nm, 5 ms)	in vivo, murine	Ovalbumin[g] [89]
2013	Fractional CO_2 (10,600 m, 16 ms)	in vivo, human	ALA[e] [90]
2013	Ti:Sapphire (801 nm, 70 fs)	in vivo, murine	ALA[e] [91]

[a]Hydrocortisone is a topical steroid for the treatment of inflammatory skin conditions
[b]Interferons are proteins which boost the immune system [92]
[c]5-Fluorouracil is an anticancer agent [79]
[d]Lidocaine is a common local anaesthetic [84]
[e]5-Aminolevulinic acid (ALA) and methyl ALA are photosensitizers used in photodynamic therapy [55, 59]
[f]Prednisone is a steroid used, for example, as an immunosuppressant [53]
[g]Ovalbumin is a model vaccine antigen [89]
[h]Diclofenac is a nonsteroidal anti-inflammatory drug [84]
[i]Anti-thymocyte globulin (ATG) and Basiliximab are proteins used for immunosuppression [85]
[j] Polyethylene glycols (PEGs) were used as high molecular weight model compounds [88]

and depth to be tailored for the application [47]. The pores created using this device are approximately 150–200 μm in diameter [47].

Adverse effects after ablation by fractional Er:YAG and CO_2 lasers include skin irritation and swelling, as well as those discussed for conventional laser ablation [55, 87, 97, 98]. Scarring has also been associated with the use of CO_2 lasers. Fewer of these symptoms are reported when fractional lasers are used [99]. The healing time after fractional or conventional laser treatment is also a concern, especially when considering multiple long-term treatments. Cost and the complex design of poration systems are considered drawbacks to their use for the enhancement of percutaneous transport [54].

The adverse side effects observed in ablation with microsecond pulses could be addressed with the use of ultra-short pulses, in the pico- or femto-second range. When these short pulses are used for tissue ablation, the laser energy is deposited and quickly transferred to kinetic energy of the ejected material, with little being transferred to the surrounding tissue, and minimal, if any, thermal damage [100]. Ideally, the laser system would be cheaper to develop and operate. The development of the technology associated with a device for ablation (cheaper laser, fibre optics) would bring down the cost of this kind of system. Also, the safety of a device, which uses a laser, can be improved with the use of visible light. As the latter can be detected by eye, it is much easier to avoid any unintentional exposures and harmful effects.

2.4.3.1 Ablation with Visible Wavelengths and Femtosecond Pulses

There have been few reported uses of visible laser light (400–700 nm) poration for enhanced drug delivery. At visible wavelengths, melanin and haemoglobin are the skin chromophores that have the greatest absorption capabilities. This means that the absorption of visible laser light at longer pulse lengths by skin depends on its pigmentation. Visible wavelengths are used, for example, in tattoo removal [101] and the treatment of pigmented lesions [62]. The use of a frequency doubled Nd:YAG laser (λ = 532 nm) with nanosecond pulses has been reported to enhance the delivery of 5-fluorouracil [81] and 5-aminolevulinic acid (ALA) [59]. In the first of these studies [81], irradiation at 532 nm was found to enhance the delivery of 5-fluorouracil, compared to its penetration across untreated skin, with no visible damage to the surrounding skin. At a given fluence, the enhancement at wavelengths of 355 and 1064 nm was greater, but damaging effects on the tissue surrounding the pores were observed. In a separate study, a lower fluence from an Er:YAG laser was required to enhance ALA delivery compared to that needed by a frequency doubled Nd:YAG laser with a wavelength of 532 nm [59]. Histological studies again showed no damage to the skin was caused by irradiation with the 532 nm laser.

Pulse lengths on the order of tens of femtoseconds have been used to ablate, for example, the cornea [102], teeth [103], skin [104, 105] and neural tissue [106]. The plasma mediated ablation, which occurs when ultrashort (pico- and femto-second) pulse durations are used, is often associated with the generation of stress that causes tissue damage [107]. In principle, the expansion of plasma, formed by laser

irradiance, leads to the propagation of a shock wave through the tissue. However, the shock wave produced by femtosecond pulses has extremely high frequency and cannot propagate through tissue, being entirely absorbed in a subsurface layer less than 1 μm in thickness [107]. There is a paucity of literature describing the use of femtosecond pulsed lasers to enhance the permeation of therapeutic agents into and across the skin. Nicolodelli et al. [91] porated skin using a Ti:Sapphire laser (λ = 801 nm) with a pulse length of 70 fs and found that this enhanced the depth of ALA in the skin. Thermal damage, however, was observed surrounding the pores.

The optical absorption of the skin at 532 nm is low [56]. Greater fluences are therefore required for laser induced breakdown as seed electrons are not so easily produced at this wavelength. The absorption of the green light can be enhanced by applying a strongly absorbing dye to the surface of the skin. This effect has been investigated [108] using pulse lengths from 50 to 200 ms. Carbon particles mixed with film forming polymers provided the means by which green light was absorbed and converted to thermal energy. The presence of the dye induced tissue ablation but thermal injury was observed in a band of collagen denaturation in the surrounding tissue. The use of carbon suspensions to enhance laser treatment of acne and facial pores with a 1064 nm laser [109, 110] has been reported but there are no examples of its use to enhance drug delivery.

There has been no reported use of ablation of dyed skin using a visible laser with femtosecond pulses. The mechanism of ablation deriving from this combination is of interest to the efficient delivery of vaccines, proteins, peptides and smaller drug molecules into and across the skin.

References

1. H. Schaefer, T.E. Redelmeier, *Skin Barrier: Principles of Percutaneous Absorption* (Karger, Basel, New York, 1996)
2. D.H. Kim, N.S. Lu, R. Ma, Y.S. Kim, R.H. Kim, S.D. Wang, J. Wu, S.M. Won, H. Tao, A. Islam, K.J. Yu, T.I. Kim, R. Chowdhury, M. Ying, L.Z. Xu, M. Li, H.J. Chung, H. Keum, M. McCormick, P. Liu, Y.W. Zhang, F.G. Omenetto, Y.G. Huang, T. Coleman, J.A. Rogers, Epidermal electronics. Science **333**(6044), 838–843 (2011)
3. A. Williams, *Transdermal and Topical Drug Delivery from Theory to Clinical Practice* (Pharmaceutical Press, London, 2003)
4. C. Ehrhardt, K. Kim, Drug Absorption Studies : in Situ, in Vitro and in Silico Models. Biotechnology : Pharmaceutical Aspects (Springer, New York, 2008)
5. P.M. Elias, Epidermal lipids, membranes, and keratinization. Int. J. Dermatol. **20**(1), 1–19 (1981)
6. R.J. Scheuplein, A personal view of skin permeation (1960–2013). Skin Pharmacol. Physiol. **26**(4–6), 199–212 (2013)
7. R.H. Guy, Skin—'that unfakeable young surface'. Skin Pharmacol. Physiol. **26**(4–6), 181–189 (2013)
8. A.V. Rawlings, I.R. Scott, C.R. Harding, P.A. Bowser, Stratum-corneum moisturization at the molecular-level. J. Invest. Dermatol. **103**(5), 731–740 (1994)
9. N. Sekkat, Y.N. Kalia, R.H. Guy, Porcine ear skin as a model for the assessment of transdermal drug delivery to premature neonates. Pharm. Res. **21**(8), 1390–1397 (2004)

10. K.C. Madison, Barrier function of the skin: "la raison d'etre" of the epidermis. J. Invest. Dermatol. **121**(2), 231–241 (2003)
11. M.B. Delgado-Charro, R.H. Guy, Effective use of transdermal drug delivery in children. Adv. Drug Delivery Rev. **73**, 63–82 (2014)
12. V.V. Ranade, J.B. Cannon, *Drug Delivery Systems*, 3rd edn. (CRC Press, Boca Raton, 2011)
13. M.R. Prausnitz, R. Langer, Transdermal drug delivery. Nat. Biotech. **26**(11), 1261–1268 (2008)
14. J.D. Bos, M.M.H.M. Meinardi, The 500 dalton rule for the skin penetration of chemical compounds and drugs. Exp. Dermatol. **9**(3), 165–169 (2000)
15. R. Scheuplein, L. Ross, Effects of surfactants and solvents on the permeability of epidermis. J. Soc. Cosmet. Chem. **21**(13), 853–873 (1970)
16. B.G. Saar, L.R. Contreras-Rojas, X.S. Xie, R.H. Guy, Imaging drug delivery to skin with stimulated raman scattering microscopy. Mol. Pharm. **8**(3), 969–975 (2011)
17. N.B. Shelke, M. Sairam, S.B. Halligudi, T.M. Aminabhavi, Development of transdermal drug-delivery films with castor-oil-based polyurethanes. J. Appl. Polym. Sci. **103**(2), 779–788 (2007)
18. K. Frederiksen, R.H. Guy, K. Petersson, Formulation considerations in the design of topical, polymeric film-forming systems for sustained drug delivery to the skin. Eur. J. Pharm. Biopharm. **91**, 9–15 (2015)
19. M. Donkerwolcke, F. Burny, D. Muster, Tissues and bone adhesives—historical aspects. Biomaterials **19**(16), 1461–1466 (1998)
20. D.K. Jeng, A new, water-resistant, film-forming, 30-second, one-step application iodophor preoperative skin preparation. Am. J. Infect. Control **29**(6), 370–376 (2001)
21. J. Stephen-Haynes, C. Stephens, Evaluation of clinical and financial outcomes of a new no-sting barrier film and barrier cream in a large uk primary care organisation. Int. Wound J. **10**(6), 689–696 (2013)
22. I.Z. Schroeder, P. Franke, U.F. Schaefer, C.M. Lehr, Delivery of ethinylestradiol from film forming polymeric solutions across human epidermis in vitro and in vivo in pigs. J. Controlled Release **118**(2), 196–203 (2007a)
23. A. Misra, R.S. Raghuvanshi, S. Ganga, M. Diwan, G.P. Talwar, O. Singh, Formulation of a transdermal system for biphasic delivery of testosterone. J. Controlled Release **39**(1), 1–7 (1996)
24. C. Padula, G. Colombo, S. Nicoli, P.L. Catellani, G. Massimo, P. Santi, Bioadhesive film for the transdermal delivery of lidocaine: in vitro and in vivo behavior. J. Controlled Release **88**(2), 277–285 (2003)
25. H.O. Ammar, M. Ghorab, A.A. Mahmoud, T.S. Makram, A.M. Ghoneim, Rapid pain relief using transdermal film forming polymeric solution of ketorolac. Pharm. Dev. Technol. **18**(5), 1005–1016 (2013)
26. I.Z. Schroeder, P. Franke, U.F. Schaefer, C.M. Lehr, Development and characterization of film forming polymeric solutions for skin drug delivery. Eur. J. Pharm. Biopharm. **65**(1), 111–121 (2007b)
27. X. Tan, S.R. Feldman, J.W. Chang, R. Balkrishnan, Topical drug delivery systems in dermatology: a review of patient adherence issues. Expert Opin. Drug Delivery **9**(10), 1263–1271 (2012)
28. J.W. McGinity, L.A. Felton, *Aqueous Polymeric Coatings For Pharmaceutical Dosage Forms Drugs and the pharmaceutical sciences*, 3rd edn. (Informa Healthcare, New York, 2008)
29. F. Lecomte, J. Siepmann, M. Walther, R.J. MacRae, R. Bodmeier, Polymer blends used for the aqueous coating of solid dosage forms: importance of the type of plasticizer. J. Controlled Release **99**(1), 1–13 (2004)
30. D. Lunter, R. Daniels, In vitro skin permeation and penetration of nonivamide from novel film-forming emulsions. Skin Pharmacol. Physiol. **26**(3), 139–146 (2013)
31. P.J. Eaton, P. West, *Atomic Force Microscopy* (Oxford University Press, Oxford, New York, 2010)

32. R. Price, P.M. Young, Visualization of the crystallization of lactose from the amorphous state. J. Pharm. Sci. **93**(1), 155–164 (2004)
33. M.D. Louey, P. Mulvaney, P.J. Stewart, Characterisation of adhesional properties of lactose carriers using atomic force microscopy. J. Pharm. Biomed. Anal. **25**(3–4), 559–567 (2001)
34. H.Q.G. Shi, L. Farber, J.N. Michaels, A. Dickey, K.C. Thompson, S.D. Shelukar, P.N. Hurter, S.D. Reynolds, M.J. Kaufman, Characterization of crystalline drug nanoparticles using atomic force microscopy and complementary techniques. Pharm. Res. **20**(3), 479–484 (2003)
35. S. Ward, M. Perkins, J.X. Zhang, C.J. Roberts, C.E. Madden, S.Y. Luk, N. Patel, S.J. Ebbens, Identifying and mapping surface amorphous domains. Pharm. Res. **22**(7), 1195–1202 (2005)
36. Z. zur Muhlen, E. zur Muhlen, H. Niehus, W. Mehnert. Atomic force microscopy studies of solid lipid nanoparticles. Pharm. Res., **13**(9), 1411–1416 (1996)
37. M.L. Crichton, X.F. Chen, H. Huang, M.A.F. Kendall, Elastic modulus and viscoelastic properties of full thickness skin characterised at micro scales. Biomaterials **34**(8), 2087–2097 (2013)
38. B. Bhushan, W. Tang, S. Ge, Nanomechanical characterization of skin and skin cream. J. Microsc. **240**(2), 135–144 (2010)
39. R.M. Gaikwad, S.I. Vasilyev, S. Datta, I. Sokolov, Atomic force microscopy characterization of corneocytes: effect of moisturizer on their topology, rigidity, and friction. Skin Res. Technol. **16**(3), 275–282 (2010)
40. S. Sasic, *Pharmaceutical Applications of Raman Spectroscopy. Wiley Series on Technologies for the Pharmaceutical Industry*. (Wiley-Interscience, Hoboken, 2008)
41. A.C. Williams, H.G.M. Edwards, B.W. Barry, Fourier-transform raman-spectroscopy—a novel application for examining human stratum-corneum. Int. J. Pharm. **81**(2–3), R11–R14 (1992)
42. C.M. McGoverin, T. Rades, K.C. Gordon, Recent pharmaceutical applications of raman and terahertz spectroscopies. J. Pharm. Sci. **97**(11), 4598–4621 (2008)
43. F.C. Clarke, J.M. Jamieson, D.A. Clark, S.V. Hammond, R.D. Jee, A.C. Moffat, Chemical image fusion. the synergy of ft-nir and raman mapping microscopy to enable a more complete visualization of pharmaceutical formulations (vol 73, p 2157, 2001). Anal. Chem. **73**(10), 2369–2369 (2001)
44. G.L. Armstrong, H.G.M. Edwards, D.W. Farwell, A.C. Williams, Fourier transform raman microscopic study of drug distribution in a transdermal drug delivery device. Vib. Spectrosc. **11**(2), 105–113 (1996)
45. P. T. Treado, M. P. Nelson, *Raman Imaging*, vol. 2 (Wiley and Sons, Chichester, 2001), pp. 1429–1459
46. M.E. Auer, U.J. Griesser, J. Sawatzki, Qualitative and quantitative study of polymorphic forms in drug formulations by near infrared ft-raman spectroscopy. J. Mol. Struct. **661**, 307–317 (2003)
47. R. Weiss, M. Hessenberger, S. Kitzmuller, D. Bach, E.E. Weinberger, W.D. Krautgartner, C. Hauser-Kronberger, B. Malissen, C. Boehler, Y.N. Kalia, J. Thalhamer, S. Scheiblhofer, Transcutaneous vaccination via laser microporation. J. Controlled Release **162**(2), 391–399 (2012)
48. Y.G. Bachhav, A. Heinrich, Y.N. Kalia, Controlled intra- and transdermal protein delivery using a minimally invasive erbium:yag fractional laser ablation technology. Eur. J. Pharm. Biopharm. **84**(2), 355–364 (2013)
49. R.F. Donnelly, T.R.R. Singh, M.J. Garland, K. Migalska, R. Majithiya, C.M. McCrudden, P.L. Kole, T.M.T. Mahmood, H.O. McCarthy, A.D. Woolfson, Hydrogel-forming microneedle arrays for enhanced transdermal drug delivery. Adv. Funct. Mater. **22**(23), 4879–4890 (2012)
50. Yannic B. Schuetz, Aarti Naik, Richard H. Guy, Yogeshvar N. Kalia, Emerging strategies for the transdermal delivery of peptide and protein drugs. Expert opin. Drug Delivery **2**(3), 533–548 (2005)
51. T.M. Tuan-Mahmood, M.T.C. McCrudden, B.M. Torrisi, E. McAlister, M.J. Garland, T.R.R. Singh, R.F. Donnelly, Microneedles for intradermal and transdermal drug delivery. Eur. J. Pharm. Sci. **50**(5), 623–637 (2013)

52. H. Shapiro, L. Harris, F.W. Hetzel, D. Bar-Or, Laser assisted delivery of topical anesthesia for intramuscular needle insertion in adults. Lasers Surg. Med. **31**(4), 252–256 (2002)
53. J. Yu, Y.G. Bachhav, S. Summer, A. Heinrich, T. Bragagna, C. Bohler, Y.N. Kalia, Using controlled laser-microporation to increase transdermal delivery of prednisone. J. Controlled Release **148**(1), E71–E73 (2010)
54. S. Scheiblhofer, J. Thalhamer, R. Weiss, Laser microporation of the skin: prospects for painless application of protective and therapeutic vaccines. Expert Opin. Drug Delivery **10**(6), 761–773 (2013)
55. M. Haedersdal, F.H. Sakamoto, W.A. Farinelli, A.G. Doukas, J. Tam, R.R. Anderson, Fractional CO_2 laser-assisted drug delivery. Lasers Surg. Med. **42**(2), 113–122 (2010)
56. A. Vogel, V. Venugopalan, Mechanisms of pulsed laser ablation of biological tissues. Chem. Rev. **103**(2), 577–644 (2003)
57. X.H. Hu, Q.Y. Fang, M.J. Cariveau, X.N. Pan, G.W. Kalmus, Mechanism study of porcine skin ablation by nanosecond laser pulses at 1064, 532, 266, and 213 nm. IEEE J. Quant. Electron. **37**(3), 322–328 (2001)
58. J.S. Nelson, J.L. Mccullough, T.C. Glenn, W.H. Wright, L.H.L. Liaw, S.L. Jacques, Midinfrared laser ablation of stratum-corneum enhances in vitro percutaneous transport of drugs. J. Invest. Dermatol. **97**(5), 874–879 (1991)
59. C. Gomez, A. Costela, I. Garcia-Moreno, F. Llanes, J.M. Teijon, M.D. Blanco, Skin laser treatments enhancing transdermal delivery of ala. J. Pharm. Sci. **100**(1), 223–231 (2011)
60. R. Srinivasan, Ablation of polymers and biological tissue by ultraviolet-lasers. Science **234**(4776), 559–565 (1986)
61. R.R. Anderson, J.A. Parrish, Selective photothermolysis - precise microsurgery by selective absorption of pulsed radiation. Science **220**(4596), 524–527 (1983)
62. B. Brazzini, G. Hautmann, I. Ghersetich, J. Hercogova, T. Lotti, Laser tissue interaction in epidermal pigmented lesions. J. Eur. Acad. Dermatol. Venereol. **15**(5), 388–391 (2001)
63. G. Paltauf, P.E. Dyer, Photomechanical processes and effects in ablation. Chem. Rev. **103**(2), 487–518 (2003)
64. Y.G. Yingling, B.J. Garrison, Photochemical ablation of organic solids. Nucl. Instrum. Methods Phys. Res. Sect. B-Beam Interact. Mater. Atoms **202**, 188–194 (2003)
65. D.X. Hammer, R.J. Thomas, G.D. Noojin, B.A. Rockwell, P.K. Kennedy, W.P. Roach, Experimental investigation of ultrashort pulse laser-induced breakdown thresholds in aqueous media. IEEE J. Quantum Electron. **32**(4), 670–678 (1996)
66. A. Vogel, J. Noack, G. Huttman, G. Paltauf, Mechanisms of femtosecond laser nanosurgery of cells and tissues. Appl. Phys. B-Lasers Opt. **81**(8), 1015–1047 (2005)
67. P.K. Kennedy, A first-order model for computation of laser-induced breakdown thresholds in ocular and aqueous-media.1. theory. IEEE J. Quantum Electron. **31**(12), 2241–2249 (1995)
68. P.S. Tsai, P. Blinder, B.J. Migliori, J. Neev, Y.S. Jin, J.A. Squier, D. Kleinfeld, Plasma-mediated ablation: an optical tool for submicrometer surgery on neuronal and vascular systems. Curr. Opin. Biotechnol. **20**(1), 90–99 (2009)
69. A. Vogel, J. Noack, K. Nahen, D. Theisen, S. Busch, U. Parlitz, D.X. Hammer, G.D. Noojin, B.A. Rockwell, R. Birngruber, Energy balance of optical breakdown in water at nanosecond to femtosecond time scales. Appl. Phys. B-Lasers Opt. **68**(2), 271–280 (1999)
70. T.H. Maiman, Stimulated optical radiation in ruby. Nature **187**(4736), 493–494 (1960)
71. M.M. Zaret, G.M. Breinin, I.M. Siegel, H. Ripps, H. Schmidt, Ocular lesions produced by an optical maser (laser). Science **134**(348), 1525–1526 (1961)
72. L. Goldman, D.J. Blaney, D.J. Kindel, E.K. Franke, Effect of the laser beam on the skin. J. Invest. Dermatol. **40**(3), 121–122 (1963a)
73. L. Goldman, E.K. Franke, D.J. Kindel, D.J. Blaney, D. Richfield, Pathology of effect of laser beam on skin. Nature **197**(487), 912–914 (1963b)
74. L. Goldman, A. Freemond, P. Hornby, D.J. Blaney, Biomedical aspects of lasers. Jama-J. Am. Med. Assoc. **188**(3), 302–306 (1964)
75. L. Goldman, *Biomedical Aspects of the Laser: the Introduction of Laser Applications into Biology and Medicine* (Springer, Berlin, 1967)

76. S.L. Jacques, D.J. Mcauliffe, I.H. Blank, J.A. Parrish, Controlled removal of human stratum-corneum by pulsed laser. J. Invest. Dermatol. **88**(1), 88–93 (1987)
77. J.T. Walsh, T.J. Flotte, R.R. Anderson, T.F. Deutsch, Pulsed co_2-laser tissue ablation—effect of tissue-type and pulse duration on thermal-damage. Lasers Surg. Med. **8**(2), 108–118 (1988)
78. J.T. Walsh, T.J. Flotte, T.F. Deutsch, Er yag laser ablation of tissue—effect of pulse duration and tissue-type on thermal-damage. Lasers Surg. Med. **9**(4), 314–326 (1989)
79. W.R. Lee, S.C. Shen, K.H. Wang, C.H. Hu, J.Y. Fang, The effect of laser treatment on skin to enhance and control transdermal delivery of 5-fluorouracil. J. Pharm. Sci. **91**(7), 1613–1626 (2002)
80. A.J. Singer, R. Weeks, R. Regev, Laser-assisted anesthesia reduces the pain of venous cannulation in children and adults: a randomized controlled trial. Acad. Emerg. Med. **13**(6), 623–628 (2006)
81. C. Gomez, A. Costela, I. Garcia-Moreno, F. Llanes, J.M. Teijon, D. Blanco, Laser treatments on skin enhancing and controlling transdermal delivery of 5-fluorouracil. Lasers Surg. Med. **40**(1), 6–12 (2008)
82. B. Forster, A. Klein, R.M. Szeimies, T. Maisch, Penetration enhancement of two topical 5-aminolaevulinic acid formulations for photodynamic therapy by erbium:yag laser ablation of the stratum corneum: continuous versus fractional ablation. Exp. Dermatol. **19**(9), 806–812 (2010)
83. Y.G. Bachhav, S. Summer, A. Heinrich, T. Bragagna, C. Bohler, Y.N. Kalia, Effect of controlled laser microporation on drug transport kinetics into and across the skin. J. Controlled Release **146**(1), 31–36 (2010)
84. Y.G. Bachhav, A. Heinrich, Y.N. Kalia, Using laser microporation to improve transdermal delivery of diclofenac: increasing bioavailability and the range of therapeutic applications. Eur. J. Pharm. Biopharm. **78**(3), 408–414 (2011)
85. J. Yu, D.R. Kalaria, Y.N. Kalia, Erbium: yag fractional laser ablation for the percutaneous delivery of intact functional therapeutic antibodies. J. Controlled Release **156**(1), 53–59 (2011)
86. M. Hessenberger, R. Weiss, E.E. Weinberger, C. Boehler, J. Thalhamer, S. Scheiblhofer, Transcutaneous delivery of CPG-adjuvanted allergen via laser-generated micropores. Vaccine **31**(34), 3427–3434 (2013)
87. W.R. Lee, S.C. Shen, M.H. Pai, H.H. Yang, C.Y. Yuan, J.Y. Fang, Fractional laser as a tool to enhance the skin permeation of 5-aminolevulinic acid with minimal skin disruption: A comparison with conventional erbium:yag laser. J. Controlled Release **145**(2), 124–133 (2010)
88. C.S. Haak, B. Bhayana, W.A. Farinelli, R.R. Anderson, M. Haedersdal, The impact of treatment density and molecular weight for fractional laser-assisted drug delivery. J. Controlled Release **163**(3), 335–341 (2012)
89. X.Y. Chen, D. Shah, G. Kositratna, D. Manstein, R.R. Anderson, M.X. Wu, Facilitation of transcutaneous drug delivery and vaccine immunization by a safe laser technology. J. Controlled Release **159**(1), 43–51 (2012)
90. J. Lippert, R. Smucler, M. Vlk, Fractional carbon dioxide laser improves nodular basal cell carcinoma treatment with photodynamic therapy with methyl 5-aminolevulinate. Dermatol. Surg. **39**(8), 1202–1208 (2013)
91. G. Nicolodelli, D. P. Angarita, N. M. Inada, L. F. Tirapelli, V. S. Bagnato. Effect of photodynamic therapy on the skin using the ultrashort laser ablation. J. Biophotonics (2013)
92. P.A. Todd, K.L. Goa, Interferon gamma-1b—a review of its pharmacology and therapeutic potential in chronic granulomatous-disease. Drugs **43**(1), 111–122 (1992)
93. M.H. Tan, J.S. Dover, T.S. Hsu, K.A. Arndt, B. Stewart, Clinical evaluation of enhanced nonablative skin rejuvenation using a combination of a 532 and a 1,064 nm laser. Lasers Surg. Med. **34**(5), 439–445 (2004)
94. C.H. Lin, I.A. Aljuffali, J.Y. Fang, Lasers as an approach for promoting drug delivery via skin. Expert Opin. Drug Delivery **11**(4), 599–614 (2014)
95. D. Manstein, G.S. Herron, R.K. Sink, H. Tanner, R.R. Anderson, Fractional photothermolysis: a new concept for cutaneous remodeling using microscopic patterns of thermal injury. Lasers Surg. Med. **34**(5), 426–438 (2004)

96. Clinical results—P.L.E.A.S.E. professional (2014)
97. U. Paasch, M. Haedersdal, Laser systems for ablative fractional resurfacing. Expert Rev. Med. Devices **8**(1), 67–83 (2011)
98. E.M. Graber, E.L. Tanzi, T.S. Alster, Side effects and complications of fractional laser photothermolysis: experience with 961 treatments. Dermatol. Surg. **34**(3), 301–307 (2008)
99. L.R. Sklar, C.T. Burnett, J.S. Waibel, R.L. Moy, D.M. Ozog, Laser assisted drug delivery: a review of an evolving technology. Lasers Surg. Med. **46**(4), 249–262 (2014)
100. J. Neev, L.B. DaSilva, M.D. Feit, M.D. Perry, A.M. Rubenchik, B.C. Stuart, Ultrashort pulse lasers for hard tissue ablation. IEEE J. Sel. Top. Quantum Electron. **2**(4), 790–800 (1996)
101. K.M. Kent, E.M. Graber, Laser tattoo removal: a review. Dermatol. Surg. **38**(1), 1–13 (2012)
102. T. Juhasz, H. Frieder, R.M. Kurtz, C. Horvath, J.F. Bille, G. Mourou, Corneal refractive surgery with femtosecond lasers. IEEE J. Sel. Top. Quantum Electron. **5**(4), 902–910 (1999)
103. M. Dutra-Correa, G. Nicolodelli, J.R. Rodrigues, C. Kurachi, V.S. Bagnato, Femtosecond laser ablation on dental hard tissues-analysis of ablated profile near an interface using local effective intensity. Laser Phys. **21**(5), 965–971 (2011)
104. K.S. Frederickson, W.E. White, R.G. Wheeland, D.R. Slaughter, Precise ablation of skin with reduced collateral damage using the femtosecond-pulsed, terawatt titanium-sapphire laser. Arch. Dermatol. **129**(8), 989–993 (1993)
105. H. Huang, Z. X. Guo, Human dermis separation via ultra-short pulsed laser plasma-mediated ablation. J. Phys. D-Appl. Phys. **42**(16) (2009)
106. N. Suhm, M.H. Gotz, J.P. Fischer, F. Loesel, W. Schlegel, V. Sturm, J. Bille, R. Schroder, Ablation of neural tissue by short-pulsed lasers—a technical report. Acta Neurochir. **138**(3), 346–349 (1996)
107. A.A. Oraevsky, L.B. DaSilva, A.M. Rubenchik, M.D. Feit, M.E. Glinsky, M.D. Perry, B.M. Mammini, W. Small, B.C. Stuart, Plasma mediated ablation of biological tissues with nanosecond-to-femtosecond laser pulses: relative role of linear and nonlinear absorption. IEEE J. Sel. Top. Quantum Electron. **2**(4), 801–809 (1996)
108. C.C. Sumian, F.B. Pitre, B.E. Gauthier, M. Bouclier, S.R. Mordon, Laser skin resurfacing using a frequency doubled nd : yag laser after topical application of an exogenous chromophore. Lasers Surg. Med. **25**(1), 43–50 (1999)
109. J.Y. Jung, J.S. Hong, C.H. Ahn, J.Y. Yoon, H.H. Kwon, D.H. Suh, Prospective randomized controlled clinical and histopathological study of acne vulgaris treated with dual mode of quasi-long pulse and q-switched 1064-nm nd:yag laser assisted with a topically applied carbon suspension. J. Am. Acad. Dermatol. **66**(4), 626–633 (2012)
110. M.R. Roh, H.J. Chung, K.Y. Chung, Effects of various parameters of the 1064 nm nd:yag laser for the treatment of enlarged facial pores. J. Dermatol. Treat. **20**(4), 223–228 (2009)